Journal of Statistical Physics, Vol. 101, Nos. 1/2, 2000

Nanoscale Wave Patterns in Reactive Adsorbates with Attractive Lateral Interactions

M. Hildebrand[1] **and A. S. Mikhailov**[1]

Received November 29, 1999; final May 18, 2000

A model of a hypothetical surface chemical reaction with lateral interactions between adsorbed particles is investigated. It shows stationary, standing, and traveling nanoscale structures which result from the competition between reactions, diffusion, and the phase transition caused by attractive lateral interactions. Internal fluctuations destroy the coherence of traveling structures and lead to a complex dynamics of interacting traveling wave fragments in this system.

KEY WORDS: Nonequilibrium pattern formation; nonequilibrium fluctuations; heterogeneous catalysis.

1. INTRODUCTION

A characteristic property of spatially extended systems far from thermal equilibrium is that, besides stationary structures which can also be found in equilibrium systems, they may show oscillations, turbulence and various wave patterns.[1] In many situations, including surface chemical reactions,[2] such time-dependent steady patterns arise from the interplay of nonequilibrium reactions and the diffusion of reactants.[3] In this case, the characteristic length scale of appearing patterns is limited by the diffusion length of reacting particles, i.e., by the distance a molecule would pass until it undergoes a reactive collision. In typical heterogeneous catalytic reactions, such as the CO-oxidation on platinum single crystal surfaces,[4] the diffusion length of mobile adsorbed reactants lies in the micrometer range.

Recent observations with a fast scanning tunneling microscope however have shown various spatiotemporal patterns on nanoscales, well below the diffusion length.[5] The mechanism of those structures involves attractive

[1] Fritz-Haber-Institut der Max-Planck-Gesellschaft, Faradayweg 4–6, D-14195 Berlin, Germany.

0022-4715/00/1000-0599$18.00/0 © 2000 Plenum Publishing Corporation

potential interactions between adsorbed molecules, which provide the cohesion necessary to localize patterns on scales shorter than the diffusion length. If such interacting adsorbates are subject to nonequilibrium reactions, they can be regarded as an example of reactive soft matter.[6] To describe emerging patterns in such systems a continuum model is desirable which remains valid even for strong attractive lateral interactions and takes fluctuations explicitely into account because their characteristic scales are expected to be small. In a previous publication,[7] we have derived from the underlying microscopic master equation a nonlocal mesoscopic kinetic equation for reactive adsorbates which meets these requirements.

This approach has been used to investigate the formation of stationary microstructures of different morphologies in a single reactive adsorbate with attractive lateral interactions.[8] In a more recent publication,[9] a model for two different species has been presented, which shows the formation of traveling nanoscale structures. Similar propagating patterns have been observed experimentally in other systems that can be regarded as reactive soft matter, such as a metastable $NaNO_3$ layer formed in the reaction of single-crystal NaCl(100) with dry HNO_3 that was exposed to water[10] or thin Langmuir–Blodgett films under the influence of light-induced trans–cis isomerizations.[11] Moreover, similar traveling structures can be expected in polymer systems subject to light-induced reactions, where so far only stationary microstructures have been predicted theoretically[12] and observed experimentally.[13]

The aim of this paper is to present new results of our investigations of the previously proposed model.[9] In Section 2 the model is discussed. In Section 3 a linear stability analysis for uniform stationary states is performed. Results of numerical simulations are presented in Section 4. Finally, an outline of the derivation of the model is given in the Appendix.

2. THE MODEL

We consider a model system with two adsorbed species (U and V) that participate in a nonequilibrium annihilation reaction $U+V\rightarrow 0$. We assume that particles U are strongly attracting each other and, in absence of the other species V, this adsorbate would undergo a first-order phase transition. The particles of the second species V are attracted to particles U but do not interact between themselves. The particles V are strongly chemisorbed in comparison to the species U which is highly mobile and can desorb, in contrast to the species V. Moreover, the particles U and V occupy different sets of adsorption sites. Assuming linear transition rates, the following mesoscopic evolution equations for the fluctuating coverages

u and v can be derived through coarse graining of the microscopic master equation:

$$\begin{aligned}\frac{\partial u}{\partial t} &= k_{ad}^{u} p_u (1-u) - k_{des}^{u}(W)\, u - k_r uv + D\,\nabla^2 u \\ &\quad + \nabla\left[\frac{D}{k_B T}\, u(1-u)\,\nabla W(\mathbf{r})\right] + \xi_u(\mathbf{r}, t) \\ \frac{\partial v}{\partial t} &= k_{ad}^{v} p_v (1-v) - k_r uv + \xi_v(\mathbf{r}, t)\end{aligned} \tag{1}$$

Here k_{ad}^{u} and k_{ad}^{v} are the sticking coefficients of the species U and V, p_u and p_v are their constant partial pressures in the gas phase, k_r is the reaction rate constant, D is the diffusion constant of the mobile species U, and T is the temperature. The desorption rate coefficient $k_{des}^{u}(W)$ for the particles of type U depends on the local potential $W(\mathbf{r})$ as $k_{des}^{u}(W) = k_{des}^{u} \exp[\, W(\mathbf{r})/k_B T\,]$. This potential acting on adsorbed particles U results from attractive pairwise interactions with surrounding molecules of the species U and V and is given by

$$W(\mathbf{r}) = -\int w_{uu}(\mathbf{r}-\mathbf{r}')\, u(\mathbf{r}')\, d\mathbf{r}' - \int w_{uv}(\mathbf{r}-\mathbf{r}')\, v(\mathbf{r}')\, d\mathbf{r}' \tag{2}$$

For simplicity we assume that both binary interactions have a Gaussian profile with the same radius r_0, though their strengths are different. The interactions are therefore described by functions

$$w_{uu}(r) = \frac{w_{uu}^{0}}{\pi r_0^2} \exp\left(-\frac{r^2}{r_0^2}\right), \qquad w_{vv}(r) = \frac{w_{vv}^{0}}{\pi r_0^2} \exp\left(-\frac{r^2}{r_0^2}\right) \tag{3}$$

Note that, besides the diffusion term, the evolution equation for the mobile species U also contains a term describing drift of this adsorbed species in the gradient of the local potential. The local reaction rate constant k_r is not affected by energetic interactions because the considered reaction system is far from equilibrium. The adsorbates are placed on top of a crystal substrate that can take away any excessive energy. Furthermore, the reactants U and V are supplied and the reaction product, bearing off the energy, is continuously pumped away from the gas phase.

The random terms $\xi_u(\mathbf{r}, t)$ and $\xi_v(\mathbf{r}, t)$ in the mesoscopic equations (1) take into account internal fluctuations of adsorption, desorption, reaction and diffusion processes:

$$\begin{aligned}\xi_u(\mathbf{r},t) &= Z^{-1/2}\sqrt{k^u_{ad}(1-u)}\, f_{ad}(\mathbf{r},t) \\ &\quad + Z^{-1/2}\sqrt{k^u_{des}u\exp[\,W(\mathbf{r})/k_BT\,]}\, f_{des}(\mathbf{r},t) \\ &\quad + Z^{-1/2}\sqrt{k_r uv}\, q_{react}(\mathbf{r},t) + Z^{-1/2}\nabla(\sqrt{2Du(1-u)}\,\mathbf{f}(\mathbf{r},t)) \\ \xi_v(\mathbf{r},t) &= Z^{-1/2}\sqrt{k^v_{ad}(1-u)}\, g_{ad}(\mathbf{r},t) + Z^{-1/2}\sqrt{k_r uv}\, q_{react}(\mathbf{r},t)\end{aligned} \tag{4}$$

Their presence reflects the fact that the actual microscopic dynamics of the system is discrete and stochastic, and it is only approximately described using continuous coverage variables. They are internal in the sense that they are neither caused by variations of the system parameters nor by external random forces. Retaining such internal noises allows incorporation of microscopic fluctuations into the macroscopic description for continuous coverages. Hence, Eq. (1) can loosely be viewed as a Langevin equation describing the "Brownian motion" of the macroscopic coverage under the influence of microscopic stochastic interactions. The internal noises given by Eq. (4) involve the additional parameter Z which is absent in the macroscopic limit. It specifies the lattice density, i.e., the number of lattice sites per unit surface area of the metal substrate. Note that all terms in Eq. (4) are proportional to the atomic lattice length $l_0 = 1/\sqrt{Z}$. The random forces $\mathbf{f}$, f_{ad}, f_{des}, g_{ad}, and q_{react} represent independent white noises of unit intensity. The reaction-related noises in the equations for the coverages u and v are identical because each annihilation event simultaneously changes the numbers of particles of both species.

In the Appendix we set up the microscopic master equation and show how the mesoscopic evolution equation can be derived from it by the application of a coarse graining procedure, where the system is divided into a set of boxes with characteristic size l_B. Complete diffusional mixing is assumed inside each box and hence, a master equation for the ensemble of boxes is obtained. The latter can be approximated by a multivariate Fokker–Planck equation if a single box contains a large number of adsorption sites, i.e., if the condition $Zl_B^2 \gg 1$ is satisfied. A functional Fokker–Planck equation equivalent to the continuous description Eq. (1) is applicable only for length scales much larger than l_B. Because the smallest characteristic length of the considered problem is given by the interaction radius r_0, the mesoscopic description is applicable only if the condition $r_0 \gg l_0$ is satisfied. Note, that a similar nonlocal equation without fluctuating and kinetic terms has been independently constructed for binary alloys in the limit of long-range interactions.[14]

To simplify the following analysis of the model, the dimensionless parameters $\alpha = k^u_{ad}p_u/k^u_{des}$, $\kappa = k_r/k^u_{ad}p_u$, $\beta = k^v_{ad}p_v/k_r$, $\varepsilon = w^0_{uu}/k_BT$, $\varepsilon' = w^0_{uv}/k_BT$

and $\rho_0 = r_0/L_r$ are conveniently introduced, where $L_r = (D/k_r)^{1/2}$ corresponds to the reactive diffusion length of particles U.

3. BIFURCATION ANALYSIS

We first neglect fluctuations and consider the deterministic limit of equations (1). The stationary uniform states of the system $u = u_0$ and $v = v_0$ are obtained as solutions of the equation

$$1 - u - \alpha^{-1} u \exp[-\varepsilon u - \varepsilon' v(u)] - \kappa u v(u) = 0 \tag{5}$$

where $v(u) \equiv \beta/(\beta + u)$ and $v_0 = v(u_0)$. This equation can have either a single or three different solutions. In the latter case, a dense and a dilute uniform phase coexist.

The stability of the uniform stationary states can be tested by adding small plane wave perturbations. Introducing dimensionless time $\tau = k_{ad}^u p_u t$ and dimensionless coordinate $\xi = x/L_{ad}$, where the characteristic length is $L_{ad} = (D/k_{ad}^u p_u)^{1/2}$, we substitute $u = u_0 + \delta u \exp(\gamma_k \tau + ik\xi)$ and $v = v_0 + \delta v \exp(\gamma_k \tau + ik\xi)$ into Eqs. (1) and, after linearization, arrive at the eigenvalue problem

$$k_{ad}^u p_u (\mathscr{J}(k) - \gamma_k \mathscr{E}) \begin{pmatrix} \delta u \\ \delta v \end{pmatrix} = 0 \tag{6}$$

that determines the dimensionless linear growth rates γ_k as a function of the dimensionless wavenumber k. The elements of the dimensionless 2×2 linearization matrix $\mathscr{J}(k)$ are given by

$$\begin{aligned}
\mathscr{J}_{11}(k) &= -1 + \alpha^{-1} \exp(-\varepsilon u_0 - \varepsilon' v_0)[\varepsilon u_0 \exp(-\tfrac{1}{4} r_0^2 k^2) - 1] - \kappa v_0 \\
&\quad - k^2 + \varepsilon u_0 (1 - u_0)\, k^2 \exp(-\tfrac{1}{4} r_0^2 k^2) \\
\mathscr{J}_{12}(k) &= -\kappa u_0 + \alpha^{-1} \varepsilon' u_0 \exp(-\varepsilon u_0 - \varepsilon' v_0) \exp(-\tfrac{1}{4} r_0^2 k^2) \\
&\quad + \varepsilon' u_0 (1 - u_0)\, k^2 \exp(-\tfrac{1}{4} r_0^2 k^2) \\
\mathscr{J}_{21}(k) &= -\kappa v_0 \\
\mathscr{J}_{22}(k) &= -\kappa(\beta + u_0)
\end{aligned} \tag{7}$$

The eigenvalues $\gamma_k^{\pm}$ obtained from Eq. (6) can be either both real or both complex. The uniform stationary state becomes unstable with respect to spatially periodic perturbations with a dimensionless wavenumber k_c when the conditions $\mathrm{Re}(\gamma_k^+) = 0$ and $d\,\mathrm{Re}(\gamma_k^+)/dk^2 = 0$ are satisfied at $k = k_c$, where γ_k^+ corresponds to the growth rate with the larger real part.

If γ_k is complex at the instability point, this is a Hopf bifurcation with broken translational symmetry (we call it the *wave bifurcation*).[9] Because we have $\mathrm{Re}(\gamma_k^+) = \mathrm{tr}[\mathscr{J}(k)]/2$, the conditions for such a bifurcation are

$$\mathrm{tr}[\mathscr{J}(k)] = 0, \qquad \frac{d\,\mathrm{tr}[\mathscr{J}(k)]}{dk^2} = 0 \tag{8}$$

They yield the following expression for the dimensionless wave number k_w of the first unstable mode:

$$k_w^2 = -\frac{1}{u_0} - \kappa(\beta + u_0) + \frac{\kappa}{2}\left(\frac{v_0}{1-u_0} + \beta + u_0\right) \times \left(1 + \sqrt{1 + \frac{16(1-u_0)}{\rho_0^2[\beta + v_0 + (1-\beta)\,u_0 - u_0^2]}}\right) \tag{9}$$

In the limit $r_0 \to 0$ and for fixed β, κ and ε, the homogeneous stationary state can either be stable for all values of α or it can become unstable with respect to spatially periodic perturbations for $\alpha = \alpha_c^-$ and it can either remain unstable for all $\alpha > \alpha_c^-$ or become stable again at $\alpha = \alpha_c^+$. In this limit, the homogeneous steady state coverage u_0 equals $u_D = (1 \pm \sqrt{1 - 4/\varepsilon})/2$ at the respective boundaries of the unstable region. Expanding k_w from Eq. (9) for $\rho_0 = r_0/L_r \ll 1$ we obtain for the wavelength of the first unstable mode in nonrescaled units the following expression to the lowest order in ρ_0

$$\lambda_w = (2\pi^2)^{1/2}\left[\frac{\beta}{(1-u_D)(\beta + u_D)} + \beta + u_D\right]^{-1/4}\sqrt{r_0 L_r} \tag{10}$$

Because $\lambda_w \sim \sqrt{r_0 L_r}$, in this limit the critical wavelength λ_w would generally lie between the radius r_0 of the lateral interactions and the characteristic diffusion length of the reaction L_r. This corresponds to the submicrometer range for typical surface chemical reactions.

If the interaction radius r_0 is large enough and the characteristic intensity ε' of the cross-species interactions is sufficiently small, the growth rate γ_k^+ becomes real at the instability point. This case corresponds to a *Turing-like bifurcation* leading to the formation of stationary microstructures with some dimensionless wavenumber k_t.[8] Then we have $\mathrm{Re}(\gamma_k^+) = \gamma_k^+$ and

$$2\gamma_k^+ = \mathrm{tr}[\mathscr{J}(k)] + \{(\mathrm{tr}[\mathscr{J}(k)])^2 - 4\det[\mathscr{J}(k)]\}^{1/2} \tag{11}$$

so that this dimensionless wavenumber is given by

$$k_t^2 = -\frac{1}{u_0} - \frac{\kappa}{\beta} u_0 v_0^2 + \frac{\kappa}{2}\left(\frac{v_0}{1-u_0} - \frac{u_0 v_0^2}{\beta}\right) \times \left(1 + \sqrt{1 + \frac{16(1-u_0)}{\rho_0^2[v_0 - (1-u_0)\, u_0 v_0^2/\beta]}}\right) \tag{12}$$

Note that in the limit $\beta \to \infty$, $\varepsilon' \to 0$ this expression reduces to the one previously obtained in ref. 8 for a system with a single reactive species. For small interaction radius r_0, the wavelength of the first Turing-unstable mode is approximately

$$\lambda_t = 2^{1/2}\pi \left[\frac{\beta}{(1-u_D)(\beta+u_D)} - \frac{\beta u_D}{(\beta+u_D)^2}\right]^{-1/4} \sqrt{r_0 L_r} \tag{13}$$

It should be noted that even in the special codimension-2 situation, when the wave bifurcation and the Turing-like bifurcation take place simultaneously, the characteristic wavenumbers k_t and k_w of the respective first unstable modes are different.

Figure 1 displays instability boundaries in the parameter plane (α, ε) for several different values of the interaction radius r_0 at a fixed intensity ε' of interaction between the two species. If the interaction radius is sufficiently small, the boundary of the unstable region always corresponds to a wave bifurcation. As r_0 is increased, this boundary moves upwards. We show in Fig. 1 the boundaries of wave bifurcations for $(D/k_{des}^u)^{-1/2} r_0 = 0$, 0.02, 0.1 and 0.5. Moreover, the boundary of the Turing-like instability at $(D/k_{des}^u)^{-1/2} r_0 = 0.5$ is also shown here. The uniform stationary state is linearly unstable with respect to nonuniform spatial perturbations in the regions above the respective lines. Note that at sufficiently high α the Turing-like instability precedes the wave bifurcation.

To illustrate the transition from the wave bifurcation to the Turing-like instability, Fig. 2 additionally displays instability boundaries in the parameter plane (α, ε') for $(D/k_{des}^u)^{-1/2} r_0 = 0.025$. The solid lines indicate the wave bifurcation, while the dashed lines correspond to the Turing-like instability. The unstable region is located in the middle, between the left and the right lines. The inset (a) shows the dispersion relation for the codimension-2 situation where the uniform phase simultaneously undergoes a wave bifurcation and a Turing-like instability. In the inset (b) the uniform stationary state is unstable only with respect to a band of stationary modes and the formation of stationary microstructures can be expected. On the other hand, in the inset (c) it is unstable only with respect to a

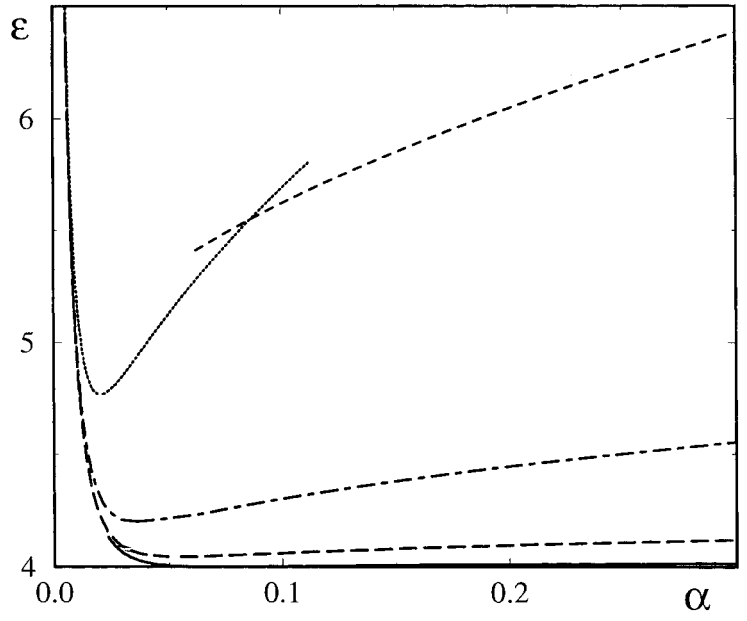

Fig. 1. Bifurcation diagrams for the uniform stationary state in the parameter plane (α, ε) for $\beta = \varepsilon' = 3$, $\kappa = 1$ and different values of the interaction radius r_0. The wave bifurcation boundary is marked by the solid line in the limit $r_0 \to 0$, and by the long-dashed, the dot-dashed, and the dotted lines for $r_0 = 0.02(D/k^u_{des})^{1/2}$, $r_0 = 0.1(D/k^u_{des})^{1/2}$, and $r_0 = 0.5(D/k^u_{des})^{1/2}$, respectively. The dashed line corresponds to the Turing-like bifurcation for $r_0 = 0.5(D/k^u_{des})^{1/2}$.

band of oscillatory modes and hence non-stationary waves will be formed. In the inset (d) the uniform stationary state is unstable with respect to both stationary and oscillatory modes. In this case the choice of the initial conditions determines whether stationary or non-stationary patterns are formed. Note that the characteristic wave number for the wave bifurcation is always larger than that for the Turing-like bifurcation, as directly follows from Eqs. (9) and (12).

The critical values of the dimensionless cross-species interaction intensity ε', where different bifurcations end and where they intersect, can be analytically calculated in the limit $\rho_0 \to 0$. The end points $\varepsilon'_{crit,\,w}$ of the wave bifurcations are determined by the conditions $\mathrm{tr}[\mathscr{J}(k_w)] = O(\rho_0)$ and $\det[\mathscr{J}(k_w)] = O(\rho_0)$ and are approximately given by

$$\varepsilon'_{crit,\,w} = \frac{\varepsilon\kappa}{\beta k_w^2}\left[(\beta + u_D)^3 + \beta u_D\right] \tag{14}$$

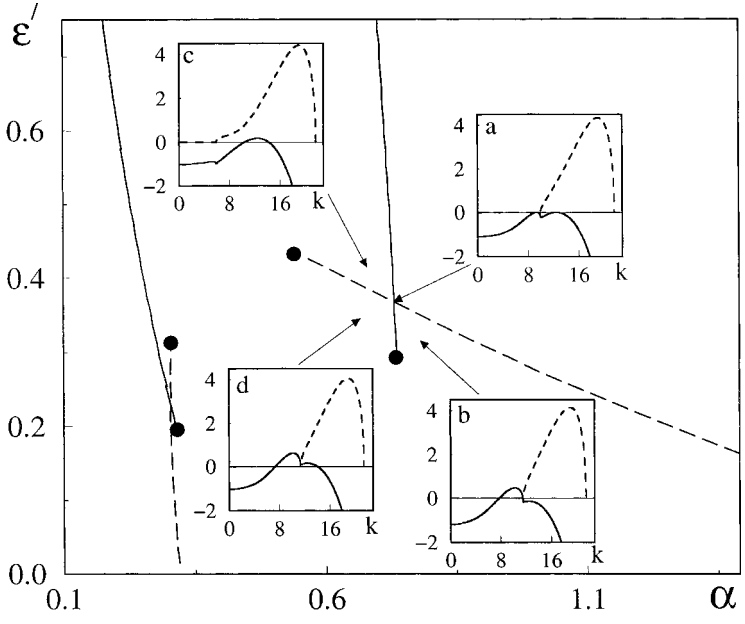

Fig. 2. Bifurcation diagram in the parameter plane (α, ε') for $\beta = 3$, $\kappa = 1$, $\varepsilon = 4.2$, and $r_0 = 0.025(D/k^u_{des})^{1/2}$. The dashed and solid lines correspond to Turing-like and wave bifurcations of the uniform stationary state respectively. The uniform phase is unstable in the parameter region bounded by the left-most and the right-most of these lines. The black dots mark the end points of the instabilities. The insets display the dispersion relations at the points marked by the arrows; (a)–(d) correspond to $\alpha = 0.73$ and $\varepsilon' = 0.368$, $\alpha = 0.78$ and $\varepsilon' = 0.315$, $\alpha = 0.667$ and $\varepsilon' = 0.415$, and $\alpha = 0.679$ and $\varepsilon' = 0.346$, respectively. The bold solid lines in the insets correspond to the real part of the eigenvalues γ_k^+, the dashed lines to their imaginary parts in dependence of the dimensionless wave number k.

The end point $\varepsilon'_{crit,\,t}$ of the Turing-like bifurcation is determined by $\mathrm{tr}[\mathscr{J}(k_t)] = O(\rho_0)$ and $\det[\mathscr{J}(k_t)] = O(\rho_0)$, and is approximately

$$\varepsilon'_{crit,\,t} = \frac{\varepsilon\kappa}{\beta k_t^2}\left[(\beta + u_D)^3 + \beta u_D\right] \tag{15}$$

The critical value ε'_{tw} corresponding to the codimension-2 situation, where the wave and the Turing-like bifurcations cross (i.e., the solid and the dashed lines in Fig. 2 intersect), is determined by simultaneously requiring that $\mathrm{tr}[\mathscr{J}(k_w)] = O(\rho_0)$, and $d\,\mathrm{tr}[\mathscr{J}(k_w)]/dk^2 = O(\rho_0^2)$, and that

$\det[\mathscr{J}(k_t)] = O(\rho_0)$, and $d\det[\mathscr{J}(k_t)]/dk^2 = O(\rho_0^2)$. It is approximately given by

$$\varepsilon'_{tw} = \frac{2\varepsilon\kappa}{\beta(k_t^2 + k_w^2)} [(\beta + u_D)^3 + \beta u_D] \tag{16}$$

Note that we always have $\varepsilon'_{crit,\,w} < \varepsilon'_{tw} < \varepsilon'_{crit,\,t}$ in the limit $\rho_0 \ll 1$.

The selection and stability of patterns in the vicinity of the wave bifurcation can be determined by calculating the coefficients of universal coupled dynamical equations for the amplitudes of unstable modes representing left- and right-propagating waves, which are nonlocal if the group velocity is finite.[15] Such a weakly nonlinear analysis has been performed for the one-dimensional system in the absence of thermal desorption of the species U.[16] We find that for very small interaction radii the wave bifurcation is always subcritical, while for larger values of r_0 it is supercritical. In the latter case traveling wave trains are selected which are stable with respect to spatial modulations of their amplitudes. The respective weakly nonlinear analysis for the Turing-like bifurcation in the considered system has not yet been performed.

4. NUMERICAL SIMULATIONS

The system of Eqs. (1) has been numerically integrated in one and two dimensions starting with small random perturbations added to the unstable uniform state. Figure 3 displays typical results of one-dimensional simulations of the deterministic model with periodic boundary conditions. The coverage u is shown in gray scale, with darker areas corresponding to higher coverages. Close to the Turing-like bifurcation boundary, we have found stationary microstructures (Fig. 3a) with the spatial period close to the wavelength of the first unstable mode. Near the boundary of the wave bifurcation, traveling wave trains were found (Fig. 3b) whose spatial period was again close to the analytical prediction. Figure 4a shows spatial profiles of both variables u and v in such a traveling wave. We see that they are almost harmonical. Farther away from the bifurcation boundaries, other structures, such as source-and-sink pattern shown in Fig. 3c, were observed. The spatial distributions of reactants in this pattern (Fig. 4b) are not harmonical. Figure 3d shows a one-dimensional simulation for the case when traveling stripes and stationary microstructures coexist. In the beginning of the simulation the upper half of the system was covered by the traveling pattern and the lower half by the stationary structure. We find that in this case a dislocation starts to travel through the system until it relaxes to a stationary spatially periodic pattern.

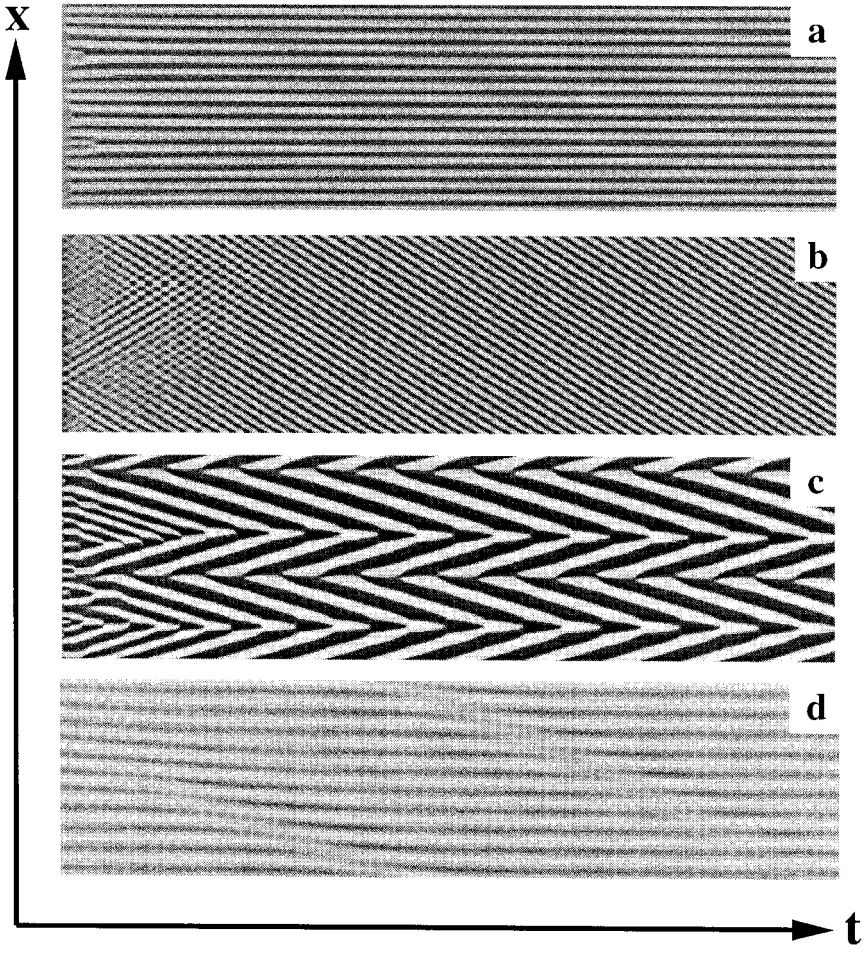

Fig. 3. Temporal evolution of the coverage $u(x, t)$ in a one-dimensional simulation of Eq. (1) in the deterministic limit for $\varepsilon = 5$, $\beta = 3$, $\kappa = 1$, $\alpha = 0.5$, $\varepsilon' = 1$ (a) resp. $\varepsilon' = 3$ (b), and $r_0 = 0.089 L_r$ in a system of size $L = 17.54 L_r$ during a time interval $T = 77/k_r$, and $\varepsilon' = 3$, $\rho_0 = 0.014$, $L = 3.89 L_r$, and $T = 8.1/k_r$ (c). As initial condition small random perturbations were added to the (unstable) uniform stationary state. In (d) special initial conditions where prepared as described in the text, the parameters where chosen as in the inset (d) of Fig. 2 with system size $L = 5.17 L_r$ and $T = 14.3/k_r$. The coverage is shown in gray scale, darker areas correspond to higher coverages.

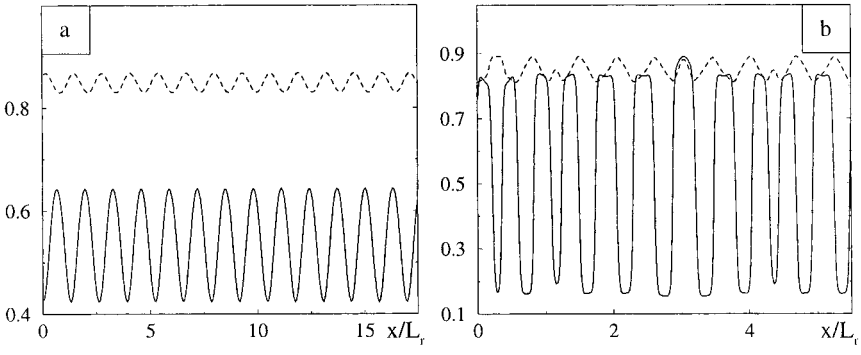

Fig. 4. One-dimensional profiles, obtained at the end of the simulations shown in Figs. 3b and 3c, respectively. The solid and dashed lines correspond to the profiles of u and v.

In the two-dimensional deterministic system we have observed standing waves consisting of oscillations between orthogonal stripe patterns, stationary microstructures, and traveling wave trains containing point-like defects.[16] These patterns are typically much smaller than the characteristic diffusion length which itself may be on the submicrometer scale. In such a

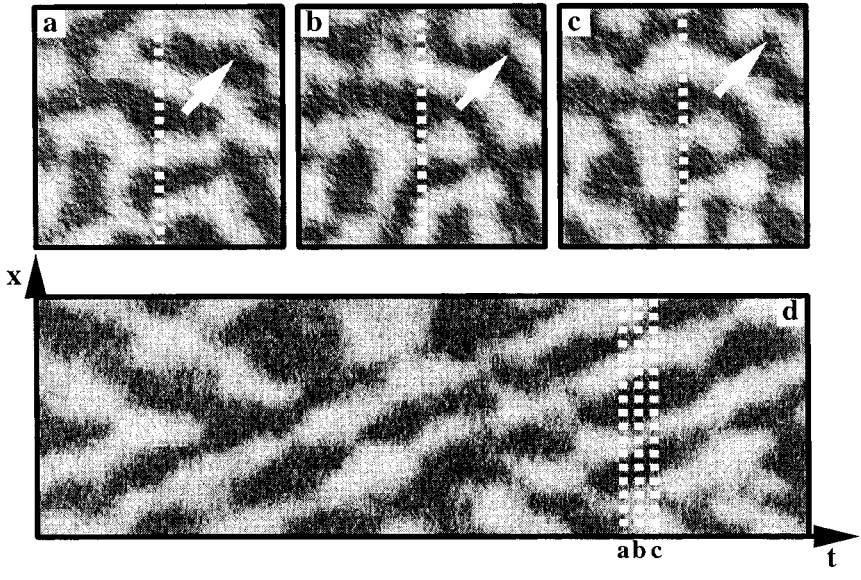

Fig. 5. Fluctuating traveling wave fragments; $Z = 1.07\,10^5\,L_r^{-2}$, $\alpha = 0.08$, $L = 1.7L_r$, $\rho_0 = 0.028$, the other parameters are the same as in Fig. 3b. The two-dimensional snapshots (a, b, c) are separated by equal intervals $\Delta t = 0.07/k_r$. The temporal evolution in the one-dimensional cross-section (d) is shown during time $T = 3.6/k_r$.

situation only a relatively small number of adsorbed particles contributes to the formation of a specific pattern and hence internal fluctuations have to be taken into account.

Figure 5 shows the fluctuating coverage distributions in the asymptotic statistical regime obtained by numerical integration of Eqs. (1) including the noise terms given by Eq. (2). Here the interaction radius r_0 is equal to only 9 atomic lattice lengths l_0, the total size of the system is $L = 555l_0$ and the characteristic diffusion length is $L_{\text{diff}} = 327l_0$. Clearly, at these small scales the internal noises of the diffusion, adsorption, desorption and reaction processes exhibit strong influence on the patterns. The individual traveling stripes are now broken into many short fragments that form irregular spatial patterns seen in the snapshots (a)–(c). Nonetheless, examining the time evolution in the central cross-section [Fig. 5d], we recognize that these fragments do not just fluctuate. These microstructures travel across the surface while undergoing irregular variations of their shapes. The directions of the translational motion of different fragments are random and the fragments often collide. Merging of traveling fragments, as well as splitting events, are observed in this process. Remarkably, the magnitude of the propagation velocity of different fragments does not significantly differ.

5. CONCLUSIONS

To summarize, we have investigated a hypothetical model where the presence of strong attractive lateral interactions in reacting adsorbates can lead to the spontaneous formation of stationary microstructures and traveling nanoscale wave fragments. Turing-like and wave bifurcations based on a comparable mechanism may be responsible for the formation of similar nonequilibrium patterns in other systems that can be regarded as reactive soft matter.

APPENDIX

The starting point for the derivation of Eqs. (1) is the microscopic lattice model. Molecules of a given adsorbate species occupy only sites of a certain planar lattice with Z lattice sites per unit area. The particles U and V occupy different sets of adsorption sites with equal density of sites. Here, this is modeled as a "stack" of two "species lattices" with identical labeling of the lattice nodes which correspond to the adsorption sites. Each site of a given species lattice can either be empty or occupied by a single particle, i.e., multiple occupation of such a site is forbidden.

Both species can arrive at a given site from the gas phase. Under the simplest assumptions, the adsorption rates, i.e., the probabilities of the arrival of a molecule from the gas phase at a given vacant site of the lattice, are $w_{ad}^{u} = k_{ad}^{u} p_u$ and $w_{ad}^{v} = k_{ad}^{v} p_v$ for particles U and V respectively, where k_{ad}^{u} and k_{ad}^{v} are the sticking coefficients and p_u and p_v correspond to the respective (constant) partial pressures in the gas phase.

While for the immobile surface species V the adsorption is the only way for a new particles to arrive at a given site, mobile particles U can arrive there also from neighboring sites of the lattice. The probability $w(\mathbf{r} \to \mathbf{r}_1)$ per unit time, that a given particle U jumps from a site $\mathbf{r}$ to a neighboring site $\mathbf{r}_1$ will in general be influenced by lateral interactions with other adsorbate molecules. The corresponding potential $W(\mathbf{r})$ experienced by the particle U at site $\mathbf{r}$ is assumed to be composed of a superposition of pairwise interactions with the surrounding adparticles, i.e., it can be expressed as

$$W(\mathbf{r}) = -\sum_{\mathbf{r}'} \left[w_{uu}(\mathbf{r} - \mathbf{r}')\, n_u(\mathbf{r}') + w_{uv}(\mathbf{r} - \mathbf{r}')\, n_v(\mathbf{r}') \right] \tag{17}$$

where $n_u(\mathbf{r}')$ and $n_v(\mathbf{r}')$ are the occupation numbers at $\mathbf{r}'$, which can take the values 0 and 1. The functions $w_{uu}(\mathbf{r})$ and $w_{uv}(\mathbf{r})$ are the binary potentials of the attractive latteral interactions between two particles which belong either to the same species U or to different species. The summation in Eq. (17) is performed over all lattice sites $\mathbf{r}'$, but because the binary potentials vanish for distances exceeding the characteristic respective interaction radii, it is actually reduced to a summation over a certain neighborhood of the site $\mathbf{r}$.

In general, $w(\mathbf{r} \to \mathbf{r}_1)$ will be a complex function of the potentials $W(\mathbf{r})$ and $W(\mathbf{r}_1)$. Here, we assume that it is determined according to the Metropolis algorithm, i.e.,

$$w(\mathbf{r} \to \mathbf{r}_1) = \nu_0 \exp\left(\frac{-H(\Delta E)\, \Delta E}{k_B T} \right) \tag{18}$$

where $\Delta E = W(\mathbf{r}_1) - W(\mathbf{r})$, ν_0 is the hopping rate of a particle U in absence of interactions, T is the surface temperature, k_B is the Boltzmann constant, and $H(z)$ corresponds to the step function, i.e., $H(z) = 1$ for $z > 0$ and $H(z) = 0$ for $z \leqslant 0$.

Besides by hopping to a neighboring site, an adsorbed particle U can leave a given site $\mathbf{r}$ by a reaction with a particle V located at $\mathbf{r}$ or by

thermal desorption. The probability per unit time for an event of the latter type, i.e., the desorption rate, is

$$w^u_{des}(\mathbf{r}) = k^u_{des} \exp\left(\frac{W(\mathbf{r})}{k_B T}\right) \tag{19}$$

where k^u_{des} is the desorption rate for a particle U occupying a site, which is isolated from any surrounding adparticles.

The probability per unit time for a reaction between a particle U and a particle V, both located at $\mathbf{r}$, is $w_r = k_r$, where k_r is the reaction rate constant. In contrast to the rate constant for thermal desorption, the latter is assumed to be independent of the potential $W(\mathbf{r})$, because the reaction takes place far from equilibrium, i.e., either it is triggered by a sufficient amount of energy directly supplied from outside, such as light, or it is strongly exothermic, i.e., the heat produced in a single reaction event is so significant that educt molecules in the vicinity of the place where such an event takes place can easily overcome the existing energy barriers for the reaction. In the latter case, the nonequilibrium situation is typically maintained by an open reaction chamber with inflowing reactands and outflowing product molecules and by removing heat from the crystal.

Using the above assumptions, a microscopic master equation for the joint probability distribution $P(\{n_u(\mathbf{r})\}, \{n_v(\mathbf{r})\}, t)$ can be set up in the following form

$$\begin{aligned}
\frac{dP}{dt} = & \sum_{\mathbf{r}} k^u_{ad} p_u \{ n_u(\mathbf{r})\, P(/n_u(\mathbf{r}) - 1/, \{n_v\}) - (1 - n_u(\mathbf{r}))\, P \} \\
& + \sum_{\mathbf{r}} k^v_{ad} p_v \{ n_v(\mathbf{r})\, P(\{n_u\}, /n_v(\mathbf{r}) - 1/) - (1 - n_v(\mathbf{r}))\, P \} \\
& + \sum_{\mathbf{r}} k^u_{des} \exp\left[\frac{W(\mathbf{r})}{k_B T}\right] \{ [1 - n_u(\mathbf{r})]\, P(/n_u(\mathbf{r}) + 1/, \{n_v\}) - n_u(\mathbf{r})\, P \} \\
& + \sum_{\mathbf{r}} k_r \{ [1 - n_u(\mathbf{r})][1 - n_v(\mathbf{r})]\, P(/n_u(\mathbf{r}) + 1/, /n_v(\mathbf{r}) + 1/) \\
& - n_u(\mathbf{r})\, n_v(\mathbf{r})\, P \} \\
& + \sum_{\mathbf{r}, \mathbf{r}_1} w(\mathbf{r}_1 \to \mathbf{r}) \{ n_u(\mathbf{r}) [1 - n_u(\mathbf{r}_1)]\, P(/n_u(\mathbf{r}) - 1, n_u(\mathbf{r}_1) + 1/, \{n_v\}) \\
& - [1 - n_u(\mathbf{r})]\, n_u(\mathbf{r}_1)\, P \}
\end{aligned} \tag{20}$$

The summation over $\mathbf{r}_1$ in the last term of this equation includes only sites that represent nearest neighbors of the site $\mathbf{r}$. The short notations

$P(/n_u(\mathbf{r}) \pm 1/, \{n_v\})$, $P(/\{n_u\}, n_v(\mathbf{r}) \pm 1/)$, and $P(/n_u(\mathbf{r}) \pm 1/, /n_v(\mathbf{r}) \pm 1/)$ are used, which mean that the set of occupation numbers in this distribution differs from that in the distribution P only at the location $\mathbf{r}$ where the occupation numbers $n_u(\mathbf{r})$, $n_v(\mathbf{r})$, and both numbers, respectively, are increased (decreased) by one. $P(|n_u(\mathbf{r})-1, n_u(\mathbf{r}_1)+1|, \{n_v\})$ denotes the probability distribution for the case when $n_u(\mathbf{r})$ and $n_u(\mathbf{r}_1)$ are decreased respectively increased by one and the other occupation numbers are identical with respect to P.

In the next step, coarse graining is introduced by dividing the lattice into a set of boxes, each containing a large number of site locations. To simplify the notations, the derivation is carried out in a one-dimensional system, but it can straightforwardly be generalized to the two-dimensional case. The system is divided into m boxes, each containing a large number $N_{\max}$ of site locations, which are still small as compared to the minimal characteristic length scale of the appearing spatial patterns. Complete diffusional mixing is assumed to take place inside every such box.

The total probabilities per unit time for the occurrence of an adsorption (of U or V particles) or a desorption event (only U) in a box j already containing $n_{u,j}$ and $n_{v,j}$ particles are proportional to the number of respective empty or occupied lattice sites in this box and are therefore given by the equations

$$\begin{aligned} \tilde{w}^{ad,u}(n_{u,j}) &= w^u_{ad}(N_{\max} - n_{u,j}) \\ \tilde{w}^{ad,v}(n_{v,j}) &= w^v_{ad}(N_{\max} - n_{v,j}) \\ \tilde{w}^{des,u}_j(n_{u,j}) &= w^{des,u}_j n_{u,j} \end{aligned} \tag{21}$$

where $w^{des,u}_j = k^u_{des}\exp(W_j/k_B T)$, assuming that the potential $W(\mathbf{r})$ does not change significantly inside the jth box, and therefore can be represented by a certain value W_j. Similarly, the total probability for the occurrence of a reaction in the jth box is

$$\tilde{w}^r(n_{u,j}, n_{v,j}) = w_r n_{u,j} n_{v,j}/N_{\max} \tag{22}$$

The mobility of adsorbed particles U is described as a random walk of particles on a chain of boxes. In the presence of potential interactions, the hopping rates of the particles are asymmetric. The probability fluxes for the jth box can be schematically represented as

$$\begin{aligned} [j-1] &\xrightarrow{\tilde{w}^+_{j-1}} [j] \xrightarrow{\tilde{w}^+_j} [j+1] \\ [j-1] &\xleftarrow{\tilde{w}^-_j} [j] \xleftarrow{\tilde{w}^-_{j+1}} [j+1] \end{aligned} \tag{23}$$

Under the assumption of complete mixing inside the boxes, the probabilities per unit time $\tilde{w}_j^{\pm}$ for a transition between the neighboring boxes are proportional to the number $n_{u,j}$ of particles in the jth box and to the fraction $1-n_{u,j\pm1}/N_{\max}$ of empty sites in the target box. Thus we have

$$\tilde{w}_j^{\pm} = w_j^{\pm}\left(1-\frac{n_{u,j\pm1}}{N_{\max}}\right) n_{u,j} \tag{24}$$

where the hopping rates for a single particle U into a free site in the adjacent box are given [cf. Eq. (18)] by

$$w_j^{\pm} = v\exp\left[\frac{(W_j - W_{j\pm1})\,H(W_{j\pm1}-W_j)}{k_B T}\right] \tag{25}$$

and v is the hopping rate between the boxes in the interaction-free case. Using these notations, we obtain the master equation for the multidimensional distribution $p(\{n_{u,1},\ldots,n_{u,m}\},\{n_{v,1},\ldots,n_{v,m}\},t)$, which gives the probability of finding $n_{u,1},\ldots,n_{u,m}$ and $n_{v,1},\ldots,n_{v,m}$ particles U resp. V in the boxes located at $x_1,\ldots,x_m$ at the time moment t (for the terms corresponding to the transport of adsorbed particles across the surface cf. ref. 7):

$$\begin{aligned}
\frac{\partial p}{\partial t} &= w_{ad}^{u}\sum_j\left[(N_{\max}-n_{u,j}+1)\,\tilde{p}_{u,j}^{-}-(N_{\max}-n_{u,j})\,p\right]\\
&+ w_{ad}^{v}\sum_j\left[(N_{\max}-n_{v,j}+1)\,\tilde{p}_{v,j}^{-}-(N_{\max}-n_{v,j})\,p\right]\\
&+\sum_j w_j^{des,u}\left[(n_{u,j}+1)\,\tilde{p}_{u,j}^{+}-n_{u,j}p\right]\\
&+\sum_j w_r\left[(n_{u,j}+1)(n_{v,j}+1)\,\hat{p}_j^{+}-n_{u,j}n_{v,j}p\right]\\
&+\sum_j \sigma_j(n_{u,j}+1)\left\{\left(1-\frac{n_{u,j+1}-1}{N_{\max}}\right)p_j^{+}+\left(1-\frac{n_{u,j-1}-1}{N_{\max}}\right)p_j^{-}\right\}\\
&-\sum_j \sigma_j n_{u,j}\left(2-\frac{n_{u,j+1}+n_{u,j-1}}{N_{\max}}\right)p\\
&+\sum_j \gamma_j(n_{u,j}+1)\left\{\left(1-\frac{n_{u,j+1}-1}{N_{\max}}\right)p_j^{+}-\left(1-\frac{n_{u,j-1}-1}{N_{\max}}\right)p_j^{-}\right\}\\
&+\sum_j \gamma_j n_{u,j}\left(\frac{n_{u,j+1}-n_{u,j-1}}{N_{\max}}\right)p
\end{aligned} \tag{26}$$

Here the sums over j are taken from 1 to m and the following short notations are employed:

$$\begin{aligned}
p &= p(\{n_{u,1},\ldots,n_{u,m}\},\{n_{v,1},\ldots,n_{v,m}\},t)\\
\tilde{p}^{\pm}_{u,j} &= p(\{n_{u,1},\ldots,n_{u,j}\pm 1,\ldots,n_{u,m}\},\{n_{v,1},\ldots,n_{v,m}\},t)\\
\tilde{p}^{-}_{v,j} &= p(\{n_{u,1},\ldots,n_{u,m}\},\{n_{v,1},\ldots,n_{v,j}-1,\ldots,n_{v,m}\},t)\\
\hat{p}^{+}_{j} &= p(\{n_{u,1},\ldots,n_{u,j}+1,\ldots,n_{u,m}\},\{n_{v,1},\ldots,n_{v,j}+1,\ldots,n_{v,m}\},t)\\
p^{+}_{j} &= p(\{n_{u,1},\ldots,n_{u,j}+1,n_{u,j+1}-1,\ldots,n_{u,m}\},\{n_{v,1},\ldots,n_{v,m}\},t)\\
p^{-}_{j} &= p(\{n_{u,1},\ldots,n_{u,j-1}-1,n_{u,j}+1,\ldots,n_{u,m}\},\{n_{v,1},\ldots,n_{v,m}\},t)\\
\sigma_j &= (w^{+}_{j}+w^{-}_{j})/2\\
\gamma_j &= (w^{+}_{j}-w^{-}_{j})/2
\end{aligned} \tag{27}$$

Now we use our assumption that the number of lattice sites $N_{\max}$ in each box is large (i.e., $N_{\max}\gg 1$). Introducing the local coverages $u_j = n_{u,j}/N_{\max}$ and $v_j = n_{v,j}/N_{\max}$ and taking into account that the coverages change only a little as a result of an adsorbtion, desorption, reaction or hopping event, that involves a single particle, we write approximately that

$$\begin{aligned}
\tilde{p}^{\pm}_{u,j} &\approx P \pm N^{-1}_{\max}\frac{\partial P}{\partial u_j}+\frac{1}{2}N^{-2}_{\max}\frac{\partial^2 P}{\partial u_j^2}\\
\tilde{p}^{-}_{v,j} &\approx P - N^{-1}_{\max}\frac{\partial P}{\partial v_j}+\frac{1}{2}N^{-2}_{\max}\frac{\partial^2 P}{\partial v_j^2}\\
\hat{p}^{+}_{j} &\approx P + N^{-1}_{\max}\left\{\frac{\partial P}{\partial u_j}+\frac{\partial P}{\partial v_j}\right\}+N^{-2}_{\max}\left\{\frac{1}{2}\frac{\partial^2 P}{\partial u_j^2}+\frac{1}{2}\frac{\partial^2 P}{\partial v_j^2}+\frac{\partial^2 P}{\partial u_j\,\partial v_j}\right\}\\
p^{\pm}_{j} &\approx P + N^{-1}_{\max}\left\{\frac{\partial P}{\partial u_j}-\frac{\partial P}{\partial u_{j\pm 1}}\right\}+N^{-2}_{\max}\left\{\frac{1}{2}\frac{\partial^2 P}{\partial u_j^2}+\frac{1}{2}\frac{\partial^2 P}{\partial u_{j\pm 1}^2}-\frac{\partial^2 P}{\partial u_j\,\partial u_{j\pm 1}}\right\}
\end{aligned} \tag{28}$$

where P is a short notation for the distribution function $P(\{u_j\},\{v_j\},t)$. Substituting these approximations into (26) and retaining there the terms up to the order $1/N_{\max}$, we obtain a multidimensional Fokker–Planck equation for the joint probability distribution $P(\{u_j\},\{v_j\},t)$ (cf. ref. 7).

As mentioned above, the size of an individual box (which is denoted below as l_B) is small as compared to the minimal characteristic scale of the considered spatial patterns. Therefore the coverages u_j and v_j do not significantly change between the neighboring boxes and can be viewed as the values of certain smooth coverages $u(x)$ and $v(x)$, respectively, taken at discrete coordinate points.

This notion allows us to introduce a continuous version of the multidimensional Fokker–Planck equation in terms of the smooth coverages $u(x)$ and $v(x)$. After the transformation to continuous coordinates, the multidimensional distribution function $P(\{u_j\}, \{v_j\}, t)$ converts into the functional $P([u(x)], [v(x)], t)$ that gives the probability density of various realizations of the random coverage fields $u(x)$ and $v(x)$. The evolution equation for this functional is

$$
\begin{aligned}
\frac{\partial P}{\partial t} = & -\int dx \frac{\delta}{\delta v(x)} \{[w_{ad}^{v}(1-v) - w_r uv]\, P\} \\
& -\int dx \frac{\delta}{\delta u(x)} \left\{ \left[w_{ad}^{u}(1-u) - w^{des,\,u} u - w_r uv - 2l_B \frac{\partial(\gamma u(1-u))}{\partial x} \right] P \right\} \\
& - l_B^2 \int dx \frac{\delta}{\delta u(x)} \left\{ \left[(1-u) \frac{\partial^2(\sigma u)}{\partial x^2} + \sigma u \frac{\partial^2 u}{\partial x^2} \right] P \right\} \\
& + \frac{1}{2Z} \int dx \frac{\delta^2}{\delta u(x)^2} \{[w_{ad}^{u}(1-u) + w^{des,\,u} u]\, P\} \\
& + \frac{1}{2Z} \int dx \frac{\delta^2}{\delta v(x)^2} \{[w_{ad}^{v}(1-v)]\, P\} \\
& + \frac{1}{2Z} \int dx \left[\frac{\delta^2}{\delta u(x)^2} + \frac{\delta^2}{\delta v(x)^2} + 2 \frac{\delta^2}{\delta u(x)\, \delta v(x)} \right] \{w_r uv P\} \\
& + \frac{l_B^2}{2Z} \int dx \frac{\delta^2}{\delta u(x)^2} \left\{ \left[(1-u) \frac{\partial^2(\sigma u)}{\partial x^2} - \sigma u \frac{\partial^2 u}{\partial x^2} \right] P \right\} \\
& + \frac{l_B}{2Z} \int dx \frac{\delta^2}{\delta u(x)^2} \left\{ \left[2\gamma u \frac{\partial u}{\partial x} - 2(1-u) \frac{\partial(\gamma u)}{\partial x} \right] P \right\} \\
& - \frac{l_B^2}{Z} \int dx \frac{\delta}{\delta u(x)} \frac{\partial^2}{\partial x^2} \left(\frac{\delta}{\delta u(x)} (1-u) \right) \{\sigma u P\} \\
& - \frac{l_B}{Z} \int dx \frac{\partial}{\partial x} \left(\left[\frac{\delta}{\delta u(x)} \right]^2 \right) \{\gamma u(1-u)\, P\}
\end{aligned}
\tag{29}
$$

where we have introduced the parameter $Z = N_{\max}/l_B$ that gives the number of lattice sites per unit area.

The coefficients σ and γ in Eq. (29) represent certain functions of the coordinate x that are given by the equations [cf. Eqs. (25) and (27)]

$$\sigma(x) = \frac{v}{2}\left[1 + \exp\left[-l_B \left|\frac{\partial W}{\partial x}\right| \Big/ k_B T\right]\right]$$
$$\gamma(x) = -\frac{v}{2}\left[1 - \exp\left[-l_B \left|\frac{\partial W}{\partial x}\right| \Big/ k_B T\right]\right] \operatorname{sign}\left(\frac{\partial W}{\partial x}\right) \tag{30}$$

In the limit $l_B/r_0 \to 0$ we therefore obtain

$$\lim_{l_B \to 0} (\sigma(x)\, l_B^2) = D$$
$$\lim_{l_B \to 0} (\gamma(x)\, l_B) = \lim_{l_B \to 0} \left(-\frac{v l_B^2}{2k_B T}\frac{\partial W}{\partial x}\right) = -\frac{D}{2k_B T}\frac{\partial W}{\partial x} \tag{31}$$

where

$$D = \lim_{l_B \to 0} (v l_B^2) \tag{32}$$

is the diffusion constant.

Taking Eq. (29) in the limit $l_B/r_0 \to 0$ and performing certain transformations of the transport terms (cf. ref. 7), we obtain the functional Fokker–Planck equation

$$\begin{aligned}
\frac{\partial P}{\partial t} = &-\int dx \frac{\delta}{\delta u(x)} \left\{\left[w_{ad}^u (1-u) - w^{des,\,u}(x)\, u - w_r uv \right.\right. \\
&\left.\left. + \frac{D}{k_B T}\frac{\partial}{\partial x}\left(u(1-u)\frac{\partial W}{\partial x}\right) + D\frac{\partial^2 u}{\partial x^2}\right] P\right\} \\
&-\int dx \frac{\delta}{\delta v(x)} \left\{\left[w_{ad}^v (1-v) - w_r uv \right] P\right\} \\
&+\frac{1}{2Z}\int\int dx\, dy \frac{\delta^2}{\delta u(x)\, \delta u(y)} \left\{\left[(w_{ad}^u (1-u) + w^{des,\,u}(x)\, u)\, \delta(x-y) \right.\right. \\
&\left.\left. + \frac{\partial^2}{\partial x\, \partial y}(2Du(1-u)\, \delta(x-y))\right] P\right\} \\
&+\frac{1}{2Z}\int\int dx\, dy \frac{\delta^2}{\delta v(x)\, \delta v(y)} \{w_{ad}^v (1-v)\, \delta(x-y)\, P\} \\
&+\frac{1}{2Z}\int\int dx\, dy \left[\frac{\delta^2}{\delta u(x)\, \delta u(y)} + \frac{\delta^2}{\delta u(x)\, \delta v(y)} + \frac{\delta^2}{\delta u(y)\, \delta v(x)} \right. \\
&\left. + \frac{\delta^2}{\delta v(x)\, \delta v(y)}\right] \{w_r uv\, \delta(x-y)\, P\}
\end{aligned} \tag{33}$$

As follows from the theory of random processes (cf. refs. 17 and 18), this Fokker–Planck equation is equivalent to the stochastic partial differential equation

$$\begin{aligned}
\frac{\partial u}{\partial t} &= k_{ad}^{u} p_u (1-u) - k_{des}^{u}(W)\, u - k_r uv + D\frac{\partial^2 u}{\partial x^2} \\
&\quad + \frac{\partial}{\partial x}\left[\frac{D}{k_B T} u(1-u)\frac{\partial}{\partial x} W(x)\right] + Z^{-1/2}\sqrt{k_{ad}^{u}(1-u)}\, f_{ad}(x,t) \\
&\quad + Z^{-1/2}\sqrt{k_{des}^{u} u \exp[\,W(x)/k_B T\,]}\, f_{des}(x,t) \\
&\quad + Z^{-1/2}\left\{\sqrt{k_r uv}\, q_{react}(x,t) + \frac{\partial}{\partial x}\left(\sqrt{2Du(1-u)}\, f(x,t)\right)\right\} \\
\frac{\partial v}{\partial t} &= k_{ad}^{v} p_v (1-v) - k_r uv + Z^{-1/2}\sqrt{k_{ad}^{v}(1-v)}\, g_{ad}(x,t) \\
&\quad + Z^{-1/2}\sqrt{k_r uv}\, q_{react}(x,t)
\end{aligned} \tag{34}$$

where $f_{ad}(x,t)$, $f_{des}(x,t)$, $q_{react}(x,t)$, $f(x,t)$, and $g_{ad}(x,t)$ are independent white noises of unit intensity, and the Ito interpretation of the stochastic partial differential equation is chosen.

REFERENCES

1. R. Kapral and K. Showalter, eds., *Chemical Waves and Patterns* (Kluwer, Dordrecht 1995).
2. R. Imbihl and G. Ertl, *Chem. Rev.* **95**:697 (1995).
3. A. S. Mikhailov, *Foundations of Synergetics I. Distributed Active Systems*, 2nd revised ed. (Springer, Berlin, Heidelberg, 1994).
4. S. Jakubith, H. H. Rotermund, W. Engel, A. von Oertzen, and G. Ertl, *Phys. Rev. Lett.* **65**:3013 (1990).
5. J. Wintterlin, J. Trostr, S. Renisch, R. Schuster, T. Zambelli, and G. Ertl, *Surf. Sci.* **394**:159 (1997); J. Wintterlin, S. Völkening, T. V. W. Janssens, T. Zambelli, and G. Ertl, *Science* **278**:1931 (1997); T. Zambelli, J. V. Barth, J. Wintterlin, and G. Ertl, *Nature* **390**:495 (1997).
6. A. S. Mikhailov and G. Ertl, *Science* **272**:1596 (1996).
7. M Hildebrand and A. S. Mikhailov, *J. Phys. Chem.* **100**:19089 (1996).
8. M. Hildebrand, A. S. Mikhailov, and G. Ertl, *Phys. Rev. E* **58**:5483 (1998).
9. M. Hildebrand, A. S. Mikhailov, and G. Ertl, *Phys. Rev. Lett.* **81**:2602 (1998).
10. C. D. Zangmeister and J. E. Pemberton, *J. Phys. Chem. B* **102**:8950 (1998).
11. Y. Tabe and H. Yokoyama, *Langmuir* **11**:4609 (1995).
12. S. C. Glotzer, E. A. Di Marzio, and M. Muthukumar, *Phys. Rev. Lett.* **74**:2034 (1995); M. Motoyama and T. Ohta, *J. Phys. Soc. Jap.* **66**:2715 (1997).
13. Q. Tran-Cong and A. Harada, *Phys. Rev. Lett.* **76**:1162 (1996); Q. Tran-Cong, J. Kawai, and K. Endoh, *Chaos* **9**:298 (1999).
14. G. Giacomin and J. L. Lebowitz, *Phys. Rev. Lett.* **76**:1094 (1996).

15. E. Knobloch and J. de Luca, *Nonlinearity* **3**:975; E. Knobloch, in *Patter*, *Formation in Complex Dissipative Systems*, S. Kai, ed. (World Scientific, Singapore, 1992).
16. M. Hildebrand, PhD thesis (Humboldt University, Berlin, 1999); M. Hildebrand and A. S. Mikhailov, in preparation (2000).
17. A. S. Mikhailov, *Foundations of Synergetics II. Chaos and Noise*, 2nd revised ed. (Springer, Berlin, Heidelberg, 1996).
18. G. W. Gardiner, *Handbook of Stochastic Methods* (Springer, Berlin, Heidelberg, 1985).